Study of Self-Focusing and Self-Phase-Modulation in the Picosecond-Time Regime*†

J. Reintjes‡, R. L. Carman§, and F. Shimizu#
Harvard University, Gordon McKay Laboratory, Cambridge, Massachusetts 02138
(Received 16 March 1973)

The propagation properties of a single picosecond pulse produced by a mode-locked Nd:glass laser are studied in several liquids by observing the optically induced birefringence and the changes in spectral content of the self-focused light. The spatial properties of the focal volume are studied using multiple second-harmonic (SH) probing beams which measure the induced birefringence from a single infrared pulse sequentially in many parts of the cell. These data allow a direct determination of the velocity of propagation of the high-intensity region. The formation and disappearance of high-intensity regions is also observed, as well as propagation lengths greater than 4 cm on a single pulse for the case of CS_2. Using temporally compressed SH pulses, we find that the induced birefringence is due primarily to the orientational Kerr effect in materials such as nitrobenzene and toluene. Results in CS_2 are also consistent with this mechanism and indicate that the duration of the infrared pulse in the focal volume is less than the duration of the incident pulse. The propagation properties of filaments which pass through a 1-mm glass slide are investigated, and the properties of beams which are focused within the cell by an external lens are studied. The occasional appearance of multiple filaments on some laser shots at different temporal positions in the pulse indicates the possibility of using this technique for beam wave-front diagnostics. The experimental spectra of the self-focused light were studied using beams of picosecond pulses in a number of materials, and they are all similar, showing a symmetric broadening about the laser frequency. The spectra are modulated with an interference structure which is characteristic of a phase-modulated pulse. The effective duration of the modulated pulse is consistent with the duration of the pulse in the high-intensity region as determined from the propagation data. Most of the results of the propagation and frequency-broadening experiments can be explained with a transient theory of self-focusing which results from numerical integration of the self-focusing equations with a relaxing nonlinear index. The theory, however, predicts an asymmetric frequency broadening, and therefore additional mechanisms are discussed which may account for the large amount of upshifted light which was observed.

I. INTRODUCTION

Self-focusing of Q-switched laser beams in liquids with an orientational Kerr effect has been observed by many authors.[1] The associated observation of filamentary streaks is also well documented.[2] An instantaneous response of the medium has been demonstrated to lead to moving foci.[3] Both forward-moving[4] and backward-moving[5] foci have been observed using single-longitudinal-mode exciting lasers.

More recent observations of self-focusing in liquids with small orientational Kerr constants,[6-8] as well as in solids[9] and gases,[10] demonstrate that mechanisms other than the orientational Kerr effect may be important to the self-focusing of picosecond-duration pulses. The observation of self-focusing in liquid argon[6] and the extent of the spectral broadening in solids,[9] indicate the possible presence of an electronic Kerr effect, while self-focusing in gases may be due to electronic Kerr or optical Stark effects.[10] A mode-locked ruby laser has been used to observe the spectral broadening generated in liquids with large orientational Kerr constants. The results have been interpreted in terms of librational motion of the molecules as the dominant nonlinearity.[11]

The self-focusing effect is described by the Maxwell equation

$$\nabla_\perp^2 E(r,z,t) + 2ik\left(\frac{\partial E}{\partial z} + \frac{1}{c}\frac{\partial E}{\partial t}\right) = \frac{\omega_L^2}{c^2}\epsilon_2^{NL}(|E|^2)E \tag{1a}$$

and a dielectric-response equation

$$\tau\frac{\partial \epsilon_2}{\partial t} + \epsilon_2 = \epsilon_2|E|^2, \tag{1b}$$

where the slowly varying envelope approximation has been made in Eq. (1a) and a simple relaxation equation has been used to describe the material response in Eq. (1b). In the absence of relaxation, these equations have been studied in the steady-state and quasi-steady-state regimes by many authors.[12,13] The effects of relaxation have been treated in detail elsewhere[14-16] and will be briefly summarized here.

Because of the finite response time of the nonlinear index, the leading edge of the pulse does not experience a significant nonlinear index change. Consequently, the early part of the pulse diffracts as if the medium were linear. However, because of the integral nature of the transient

response, the tendency for focusing increases further into the pulse, causing the diameter to decrease toward the back of the pulse. For a certain range of input powers, there appears to be a tendency for the numerically calculated diameter of the tail of the pulse to stabilize. Because of the inclination of the rear of the pulse to focus, the on-axis intensity undergoes considerable amplitude distortion, resulting in a pulse which is significantly shorter in the high-intensity region than the input pulse duration. In this paper the high-intensity region which develops will be called a filament.

The filament which is in the rear of the pulse is formed primarily by the nonlinear index change set up by the early portion of the pulse and therefore is expected to diffract at a rate which is determined by the larger diameter of the leading edge. Consequently, the filament is expected to propagate over a distance which is many times the linear-diffraction length of the small-scale filament. The calculations indicate that the transient solutions are completely appropriate for pulses with durations $t_p \leq 2\tau$. Consequently, it is expected that the transient theory will be applicable to experiments performed with mode-locked lasers in materials with large orientational Kerr effects possessing relaxation times longer than a few picoseconds.

For pulse durations $t_p \gg \tau$ the relaxation equation for $\Delta\epsilon$ reduces to a definition of an instantaneously responding nonlinearity almost everywhere. The remaining Maxwell equations then predict the time-dependent location of the focal points (moving-focus model). The focal points move at a velocity greater than $0.1c/n$ for the majority of a bell-shaped pulse-intensity profile. However, since the extent of the focal volume of 5-μ diam (appropriate for many liquids) is expected to be less than 100 μ, the pulse duration usually seen by a given molecule in the focal region is less than $t = 0.01\ \text{cm}/2\times10^9\ \text{cm/sec} = 5$ psec. Since this time is comparable to or shorter than the response time of the nonlinearity in many liquids, it is obvious that the transient theory applies to the light in this high-intensity region even for the longer-duration input pulse, as well as in the case of picosecond-pulse excitation. For the case of the forward-moving focus, the velocity of the focal point is always greater than the speed of light in the medium, and the material response in the high-intensity region of the focus will always be transient if molecular orientation is the dominant nonlinearity. However, the velocity of the backward-moving focus will always be sufficiently slow near its turning point that the transient theory does not apply in the region of the turning point if the pulse length is much longer than τ. In this case a steady-state focal point exists and its properties thus far have not been explored. These effects will be hard to observe because of enhanced scattering instabilities when the backward-moving focus is synchronized with either the velocity of a backward-scattered light wave or material excitation. The higher energy passing through the focal volume may also lead to a breakdown.

In addition to self-focusing the intensity-dependent refractive index leads, in general, to spectral broadening of the input light, as has been reported by many authors using multimode Q-switched lasers and mode-locked lasers.[11,17-19] Theories of phase modulation based on plane-wave approximations have been used successfully to describe the spectra produced by the multimode Q-switched lasers.[17,19] These spectra are considerably wider than the input laser spectrum and are broadened primarily on the low-frequency side. Asymmetry ratios of Stokes to anti-Stokes energy and spectral range are typically greater than ten. The frequency-broadened spectra generated with mode-locked lasers in the same materials are much more symmetric about the center frequency,[11] but otherwise similar to those obtained with the multimode Q-switched lasers. In the case of single-mode Q-switched lasers, however, little or no spectral broadening has been observed.[20]

Most of these features can readily be explained using the dynamic self-focusing theory. In the case of the single-mode laser of pulse duration long compared to the dielectric relaxation time, the forward-moving focal points travel at a velocity significantly greater than the speed of light in the medium throughout most of their evolution.[21] Consequently, the phase modulation can build up only over a distance corresponding to the instantaneous length of a single focal volume resulting in a small amount of spectral broadening.

In the case of picosecond pulses, the velocity of the focal region very quickly reaches the speed of light, increasing the time of confinement until it is limited by one or more additional mechanisms. The increased confinement time extends the path over which the phase modulation can evolve and thus provides the grounds for considerable frequency broadening.

Owing to mode beating in the multimode laser, we expect similar results here as in the picosecond-pulse case.

In this paper we describe experiments that support most of the features of the transient theory outlined above. In these experiments, the self-focusing of a single picosecond pulse from a Nd:glass mode-locked laser was studied in CS_2 in the absence of stimulated Brillouin and Raman scat-

tering. Other liquids were examined as well for comparison purposes. In Sec. II, measurements of the spatial-propagation properties of a single pulse in self-focusing materials are presented, and the importance of a slowly responding nonlinearity is established. In Sec. III, the spectral content of the light in the filaments are presented and their interpretation in terms of the transient theory is explored. In Sec. IV, the spatial and spectral characteristics are combined in order to explore the consistency of interpretation. It is found that the transient theory accounts for most of the self-focusing properties of picosecond pulses in materials with orientational Kerr effects. Some remaining problems are identified, mostly with regard to the high degree of symmetry which is observed in the broadened spectra of the filament light. Additional interactions are explained which might account for the large amount of upshifted light.

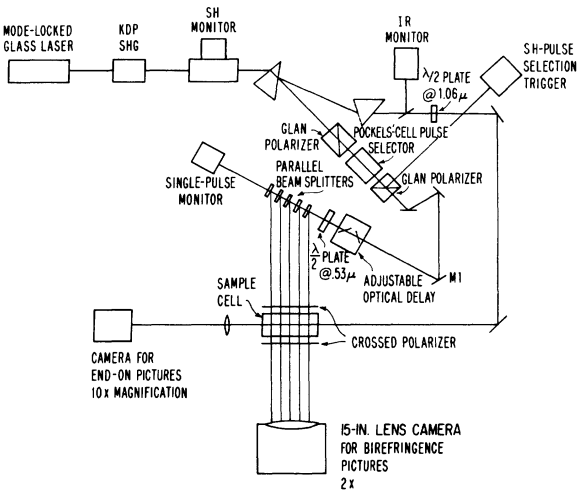

FIG. 1. Experimental configuration used to study self-focusing via observing the optically induced birefringence with five SH probing beams.

II. SPATIAL PROPAGATION PROPERTIES

In this section, a series of experiments will be described which determine the spatial-propagation properties of a single picosecond pulse in a variety of self-focusing liquids. The self-focusing of optical beams has usually been observed by photographing the beam from either the side or end of a cell containing the nonlinear medium. The usefulness of such measurements is limited because they provide information about the self-focusing process at only one point in the cell, and the results are integrated in time across an entire pulse or pulse train. Here we present results of time-resolved experiments which provide a large amount of information about the self-focusing process as it develops and about the laser pulse itself.[22] Quantities such as minimum self-focusing lengths, filament diameters, relaxation times of the dielectric nonlinearity, effective laser-pulse durations, and intensities, can be measured. In these experiments, both stimulated Raman and Brillouin scattering are observed to be absent in both the forward and backward direction, at least under the broad-band picosecond excitation, so that the processes of self-focusing and self-phase modulation can be studied without the complications introduced by other competing nonlinearities. The absence of forward-stimulated Raman scattering is unusual, but a possible explanation in terms of frequency broadening and linear-chromatic dispersion has been suggested.[23]

The technique consists of deducing the propagation characteristics of a single infrared picosecond pulse by observing the optically induced birefringence at several points in the cell. These experiments are an extension of the method introduced by Shimizu and Stoicheff,[24] and the technique is illustrated in Fig. 1. A time-of-flight measurement, performed on one infrared pulse from the laser-output-pulse train, is made possible by employing multiple probing beams, each consisting of a second-harmonic (SH) mode-locked-laser pulse.

The output of the Nd: glass mode-locked laser, with a diffraction-limited divergence for a 1-cm-diam beam, is passed through a deuterated potassium dihydrogen phosphate (KDP) SH generating crystal. The laser system and its performance will be described elsewhere. A conversion efficiency of 20% to the SH and separation by a prism results in two beams with approximately 8 mJ/pulse at 1.06 μ and 2 mJ/pulse at 0.53 μ, as is illustrated in Fig. 1. The polarization of the strong infrared beam is rotated to the vertical direction and then the beam propagates through a 20-cm-long cell filled with the self-focusing liquid. The incident laser-beam profile was somewhat degraded by the beam processing optics and KDP harmonic generator. The forward camera, which could be focused anywhere within the cell, was used to detect the presence of filaments by photographing the infrared light passing through the end of the cell at high magnification. These data were then correlated with the more precise information obtained by analyzing the induced birefringence data obtained with the multiple SH probing beams in the crossed-beam arrangement.

A single pulse is selected from the SH pulse train with a Pockels cell and is propagated through a variable optical delay. A series of beam split-

ters then produces a set of up to ten parallel SH probe beams, spaced by about 1 cm. The angles are adjusted so that the infrared and SH beams intersect at right angles in the cell. The relative timing between the first probe beam and the main infrared beam is then adjusted for coincidence using the optical delay. The pulse in each of the probe beams is timed to be coincident with the arrival of a single infrared pulse as it propagates through the cell by adjusting the angle between the infrared and SH beams at mirror $M1$. This adjustment is used to compensate for the linear refractive index of the liquid and corresponds to an angle of $23° \pm 0.05$ for CS_2. This induced birefringence is studied by placing crossed polarizers (Polaroid type HN32) in the SH beams on either side of the cell, with the axis of transmission at 45° to the vertical. The birefringence traces are photographed with a 10-in. focal length $f/4.5$ lens at a 2:1 magnification. The spatial resolution of the detection system was measured to be about 30 μ, limited chiefly by the use of type-47 Polaroid film.

Typical results are presented in Fig. 2, where the birefringence induced by a single infrared pulse is shown in successive regions throughout a 20-cm cell. Three different sources of light contribute to the photograph of each SH beam. There is leakage light from the crossed polarizers, which was measured to be 6×10^{-5} of the incident SH intensity. A second contribution is due to the change of ellipticity of the SH polarization induced by the presence of the infrared light, which remains unfocused. Finally, the desired SH signal is observed coming from the induced birefringence caused by the self-focused and filamentary infrared light. The uniformity of the laser output profile in both the infrared and green beams enables us to see birefringence due to a filament throughout the entire cross section of the SH beams, and to attribute all structure seen in the probe beams to the self-focusing process. The exception is a uniform cross hatched pattern in some of the data which was caused by one of the sets of Polaroid polarizers that were used. In addition, we can obtain either single or multiple filaments per pulse by adjusting the infrared laser intensity and beam quality. In order to obtain single filaments reliably, we found that use of a lens-aperture-lens spatial-mode selector was required in the infrared beam. This implies that the incident laser pulse does contain some spatial structure superimposed on the uniform spatial profile[25] at the cell, which is primarily due to the beam processing optics and KDP crystals. In addition, beams with diameters greater than 2 mm generally break up into multiple filaments. A discussion of this aspect of the experiments will be deferred until later in this section.

The multiple-beam technique which was used with CS_2 allows us to follow the development of a single filament through the cell. Individual filaments, which appear as streaks in the pictures, form as early as the second centimeter from the entrance window, and can be followed through at least 4 cm, as shown in Fig. 2(a). Gross beam self-focusing and breakup are also evident at the position of the first probe beam about 1 cm from the entrance window. In the 4.5–8-cm region [Fig. 2(b)], both the formation and disappearance of filaments are observed, indicating that occasionally some filaments do not travel much longer than 6 or 7 cm. In the 8–11.5-cm region [Fig. 2(c)], the filaments propagate without change in observed diameter or spatial distribution. In the 11.5–14-cm region [Fig. 2(d)], more filaments

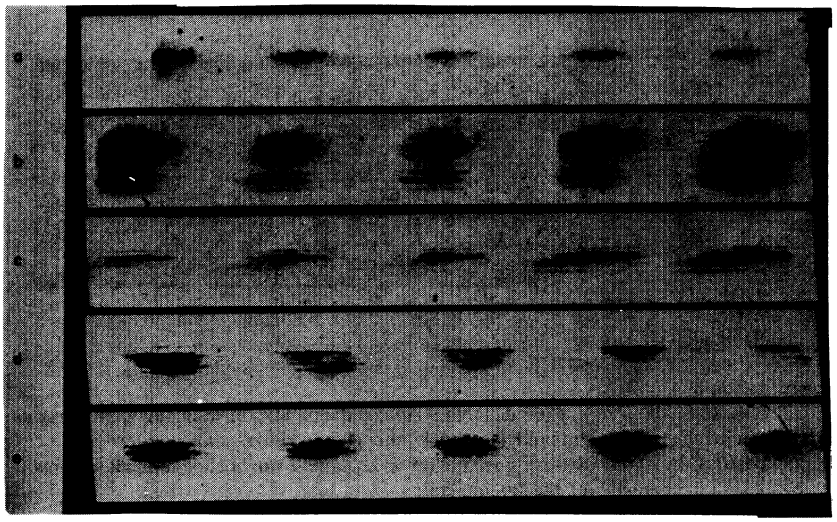

FIG. 2. Typical pictures of regions of induced birefringence in various parts of a 20-cm cell of CS_2. The infrared beam propagates from left to right. (a) 1.2 – 4.7 cm from entrance window; (b) 4.6 – 8.1 cm from entrance window; (c) 8 – 11.5 cm from entrance window; (d) 10.7 – 14.2 cm from entrance window; and (e) 15 – 18.5 cm from entrance window.

begin to disappear, while in the 15–18.5-cm region [Fig. 2(e)], almost all small-scale structure has disappeared. This indicates that laser-light filaments in CS_2 never travel much over 20 cm, when created by 1.06-μ picosecond pulses at our laser-output intensity and bandwidth, where the conditions are such that scattering is absent. The diameter of the filaments between about 4 and 12 cm is observed to be constant at the resolution limit of 30 μ, while beyond 12 cm, the filaments gradually increase in size up to as large as 100 μ.

Figure 3 shows the birefringence pattern obtained from a single probe beam positioned 5 cm from the entrance window of the CS_2 cell, as photographed with Kodak 103a J spectroscopic plates. The observed diameter of the smallest birefringence structure is 10 μ, now limited by the total SH detection-system resolution. Thus, our birefringence results are consistent with our forward-camera data and other reported measurements[7] of 4–6-μ filament diameters in CS_2.

If the delay is varied so that the SH probe beams all arrive either early or late by 15 psec, the filamentary structure disappears, while some background birefringence remains. A delay of about 100 psec on either side of coincidence is required to completely remove all detectable light due to the presence of previous infrared pulses in the pulse train, where the interpulse spacing is 10 nsec. Also, birefringence patterns that were obtained when the green probe pulse was selected from different positions in the SH pulse train, are essentially identical. Therefore, in our experiments no birefringence effects can be attributed to the previous infrared pulses in the train. The lack of cumulative effects means, in particular, that linear absorptions plays little or no role in the self-focusing process of the pulse train for CS_2. This result seems to contradict the implied conclusions of previous work, on the interaction of self-focusing and stimulated Raman scattering in the picosecond-time regime.[26,27]

In order to correlate our birefringence data with most of the existing literature, we have taken numerous pictures of the infrared beam with a camera that is focused either on or through the exit window of the CS_2 cell. Using a 6-cm-long cell, filaments of less than 10 μ in diameter in CS_2 are consistently observed, when using the standard technique of focusing on the inside surface of the exit window. When repeating this measurement for the 20-cm cell, no filaments are observed. Similar data were taken when the camera was refocused, so that the image was formed at the film from an object plane at various positions inside the cell. Results are shown in Fig. 4 for images formed at 5 and 13 cm before the exit window. The picture taken at 5 cm in front of the exit window is in agreement with the end-window picture and the birefringence data in predicting an absence of small filaments at this distance. However, the picture taken at 13 cm in front of the exit window clearly indicates the presence of filaments of less than 10 μ in diameter. Also similar pictures taken at 1 and 2 cm from the front window show absence and presence of filaments, respectively. An extensive study of this type has shown complete agreement between side (birefringence) and end (direct) pictures regarding the presence and absence of filaments crossing any particular plane in the cell. The film exposure required to photograph a filament at a distance l from the entrance window of a long cell using the above technique was observed to be comparable to the exposure required to photograph a filament at the exit window of a cell of the same length l. This important result indicates that the filaments continuously radiate a

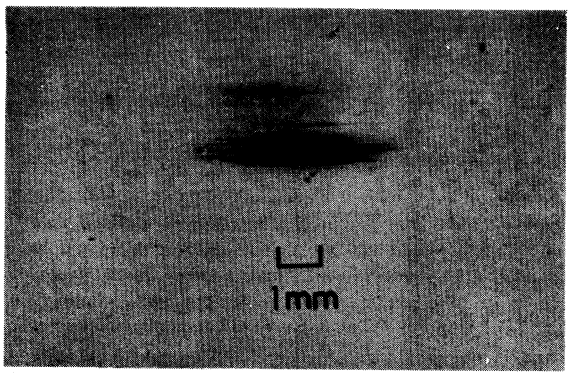

FIG. 3. Photograph of a single-probe beam taken 5 cm from the entrance window of a cell of CS_2 showing filamentary structure as small as 10 μ. Magnification of original photograph was 5× and the optical resolution was 10 μ.

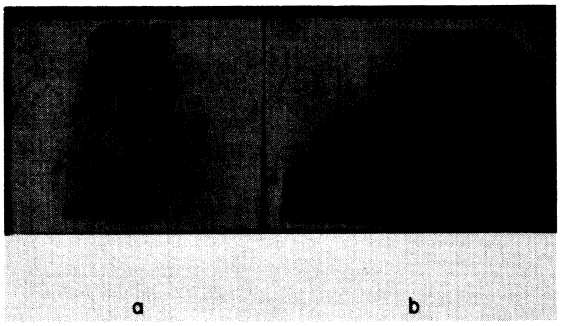

FIG. 4. Near-field pattern obtain with forward camera imaged (a) on a plane 13 cm before exit window of a 20-cm cell and (b) on a plane 7 cm before the exit window of the 20-cm cell.

significant amount of light away from the high-intensity region at large angles as they propagate.

The duration of the light in the filament can be determined with the birefringence technique through the length of the birefringence streak, in a manner similar to that of the two-photon absorption-fluorescence method of pulse-duration measurement. The length of the birefringence streak in these experiments is determined by the duration of the infrared and SH pulses and by the relaxation time of the optical anisotropy. Because the measurement is made only after the infrared beam has collapsed to its minimum diameter, the propagation time of the SH probe pulses across the infrared beam, which limited the resolution of experiments reported elsewhere,[28] is negligible here. The propagation time across a 6-μ filament is ~ 0.03 psec. The results shown in Fig. 2, where streaks last for about 25 psec, are consistent with the TPF measurements of ~ 5 psec for both SH and infrared pulse durations combined with molecular-orientation relaxation and the presence of reflections from the front and back of the parallel-face uncoated beam splitters.

In order to improve the time resolution of the birefringence measurements, the experiments were repeated using SH probing pulses which had been compressed in time by employing a grating pair,[29] in a manner similar to that introduced by Treacy.[30] In these experiments, the single pulse was selected from the infrared pulse train and amplified by a gain of ~ 8 before the KDP crystal, as shown in Fig. 5. The SH probing pulse, separated by the prism, was then consistently compressed to durations of less than 1 psec. The SH probe beam that resulted has approximately the same energy content as that which was used to obtain Fig. 2, because of the lossy nature of the grating pair. Typical results of this measurement in CS_2 are shown in Fig. 6. The front and back reflections from the beamsplitter are clearly resolved. The duration of the birefringence streaks are about 3.5–4 psec. A separation of this time into an infrared pulse duration for the filament light and a birefringence relaxation time requires refined knowledge of the self-focusing processes as well as the mechanisms which are involved.

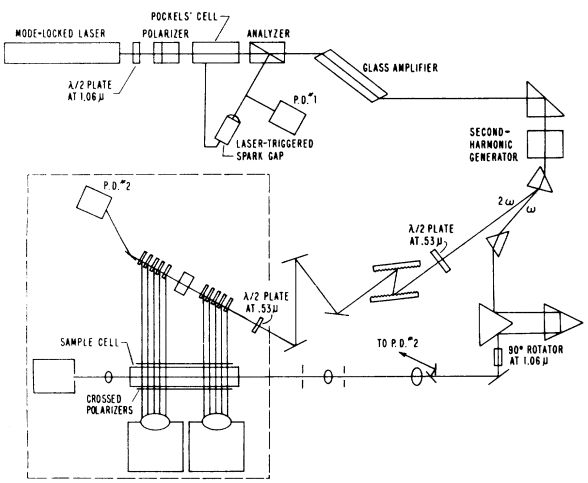

FIG. 5. Experimental configuration used to measure optically induced birefringence with improved time resolution through the introduction of a grating pair to compress the SH pulses and the use of a single amplified infrared pulse.

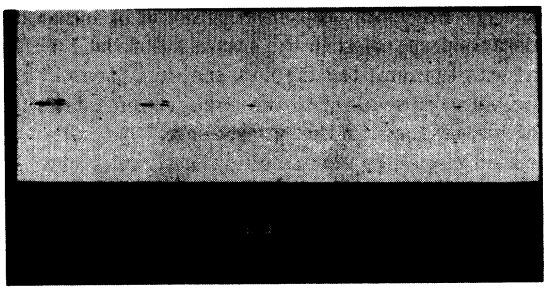

FIG. 6. Typical birefringence result in CS_2 obtained with the improved time resolution of the apparatus in Fig. 6. The reflections from the front and back surfaces of the beam splitter are clearly resolved in the first two beams.

In order to obtain further information, similar compressed SH probe-beam measurements were made in nitrobenzene, toluene, and benzene. These results have been reported in detail elsewhere[31] and will only be briefly summarized here. The results in nitrobenzene,[32] shown in Fig. 7, and in toluene indicate that the birefringence decays with a time constant equivalent to the orientational Kerr dielectric relaxation time. This result indicates that the orientational Kerr effect is important in the self-focusing of picosecond pulses even in slowly responding highly anisotropic liquids.

The results in CS_2 are also consistent with the presence of the orientational Kerr mechanism if the effective duration of the infrared pulse in the filament is about 1 psec. This time is less than the 5-psec duration of the incident infrared pulse, as determined by two-photon absorption fluorescent measurements, and is consistent both with recent calculations,[16] and with the pulse duration of the filament light predicted on the basis of the frequency broadened spectra, as will be discussed in Sec. IV. Further support for the cominance of an orientational Kerr mechanism in CS_2 is provided in Sec. IV.

Optically induced anisotropy was also observed

in CCl_4. However, the small amount of induced anisotropy resulted in the intensity of the SH light that was transmitted through the self-focused region being equivalent to the background intensity that leaked through the polarizers. The self-focused region is visible as dark streaks in a light background in the middle of the SH probing beam. The existence of the light background is probably caused by some amount of strain birefringence present in the plastic laminate of the polarizers, which is compensated for by the weak edges of the infrared pulse, causing the transmitted intensity to decrease in this region.

An accurate determination of the relaxation time of the nonlinearity in CCl_4 is difficult because of the presence of the background light. However, the streaks are visible for about 10 psec, which is much longer than the system limit indicated by the measurements in CS_2. Consequently, we conclude that the nonlinearity in CCl_4 arises at least in part from a relatively long-lived molecular interaction. A mechanism such as molecular clustering has been proposed to explain the self-focusing effect in CCl_4 by Hellwarth.[33] Competition between electronic and molecular contributions to the optically induced anisotropy has also been reported in Ref. 34. Another molecular-interaction collision-induced mechanical distortion, has been proposed as a mechanism responsible for the far-Rayleigh-wing of the spontaneous spectrum of a large number of materials, including CCl_4, and may also contribute to the self-focusing process.[35]

The experiments illustrated in Fig. 5 provide two independent means of determining the maximum value of δn that occurs in the filaments. The relative timing of successive probe beams allows a direct measurement of the propagation velocity of the high-index region. Justification for relating this velocity to the group velocity of the filament light relies on the confinement of the light in the high-intensity region, as will be discussed in detail later. Measurements in CS_2 show no detectable change in the group velocity relative to the linear value. Measurements in benzene ($n \sim 1.50$) with the probing beams timed for coincidence in CS_2 ($n \sim 1.62$) produced substantial deflections of the overlap region in the SH probe beams. The magnitude of the relative displacement of the coincidence in benzene over the five probe beams leads to an estimate that a value of $\Delta n \sim 5\times10^{-3}$ can be detected by this method. Consequently, we conclude that the nonlinear refractive index change in the filaments in CS_2 is less than the experimentally detectable limit of this method.

A more accurate method of determining the maximum index change is to compare the intensity of the SH light transmitted through the filamentary regions with the SH light that leaks through the polarizers in the absence of the infrared light. This is accomplished by using two SH beams of known intensity ratio and a calibrated neutral-density step filter, as shown in Fig. 8. The birefringence is given by

$$\delta n_{\parallel} - \delta n_{\perp} = \frac{\lambda}{\pi d}\left[\frac{2}{T^2}\left(\frac{I_s}{I_{\mathrm{inc}}} - RT\right)\right]^{1/2}, \qquad (2)$$

where $I_{\mathrm{inc}} = I_B K/RT$. In these expressions d is the diameter of the filaments, I_{inc} is the intensity of the SH light in the probing beam before the first polarizer, I_B is the background light detected by the film in the reference beam, R is the transmission ratio of a single polarizer for a beam polarized perpendicular to the axis of transmission, T is the transmission of a single polarizer polarized parallel to the axis of transmission, I_s is the intensity of the SH light that is transmitted through the polarizers due to the presence of the filamentary region, and K is the ratio of intensity between the probe and reference beams. The results obtained in CS_2 indicate that $\delta n_{\parallel} - \delta n_{\perp} = 3.3\times10^{-3}$ for a filament diameter of $6\,\mu$.[7] If the mechanism causing the induced birefringence is known, $\delta n_{\parallel}$ can be related to $\delta n_{\perp}$, allowing $\delta n_{\parallel}$ to be evaluated. The peak laser intensity can then be determined using an appropriate value of n_2. For an orientational-Kerr-effect response, $\delta n_{\parallel} = -2\delta n_{\perp}$, and therefore $\delta n_{\parallel} = 2.2\times10^{-3}$, in reasonable agreement with values determined elsewhere.[24]

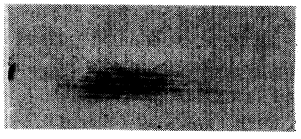

a

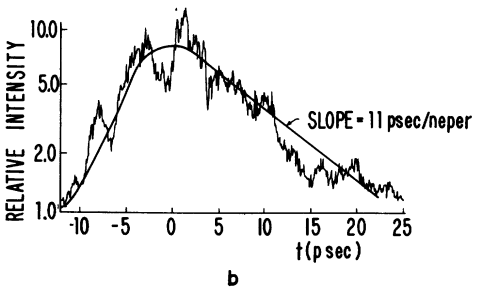

b

FIG. 7. Results of birefringence study in nitrobenzene: (a) photograph of filaments; (b) microdensitometer trace showing decay of birefringence with a time constant of 11 psec, corresponding to a lifetime of the nonlinear index of 22 ± 3 psec.

Using the transient nature of the orientational mechanism, with a ratio of relaxation time to pulse duration of 2.2, the peak optical power in the filament is then estimated to be 100 GW/cm^2.

It has been suggested that faster mechanisms, such as electron cloud distortions or librational motions, may be responsible for the nonlinear index change in many of these materials. Even if these other mechanisms are involved, the ratio of $\delta n_{\parallel}$ to $(\delta n_{\parallel} - \delta n_{\perp})$ will not differ by more than a factor of 2 or 3 from that appropriate to the orientational-Kerr-effect response. Consequently, we can conclude that the nonlinear refractive index change is far from the value that would result from complete molecular alignment even in the most intense part of the filament,[36] a result which is consistent with the conclusion of Shimizu and Stoicheff.[24] It remains to be seen if the alignment is saturating at a lower value of δn due to steric effects, as discussed by Gustafson and Townes.[37]

The effect of a glass slide on the propagation characteristics of a filament was investigated by placing a single microscope slide with a thickness of 1 mm in the infrared beam at a position between the second and third probing beams as shown in Fig. 9. Similar experiments have been used in the past in attempts to distinguish between the self-trapping and moving-focal-point theories,[38] as well as to examine the evolution of "self-trapped" beams.[39] Since a beam which is propagating in a diffractionless mode in the nonlinear medium should diffract in the much more linear $[n_2\,(\text{glass}) \sim n_2(CS_2)/100]$ glass medium, the filament would stop at the glass slide in the self-trapping model if the slide is thick compared to a diffraction length ($l_{\text{diff}} \sim 14\ \mu$ for a 6-μ-diam filament). On the other hand, the glass ($n = 1.5$) is almost index matched from a linear viewpoint

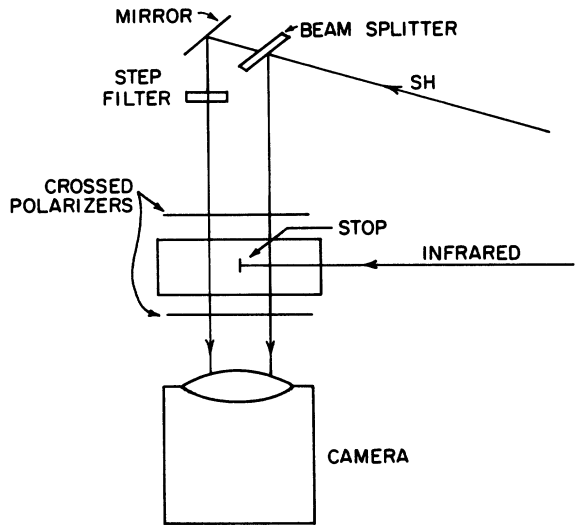

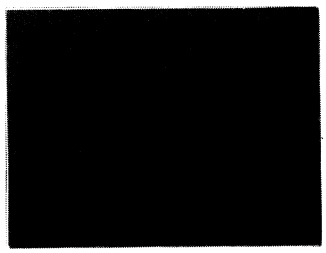

b

FIG. 8. Measurement of the maximum value of δn in the filaments: (a) experimental configuration, showing changes from basic experiments of Fig. 5 (elements in dotted box of Fig. 5 are changed to those shown); (b) results of birefringence measurements in CS_2.

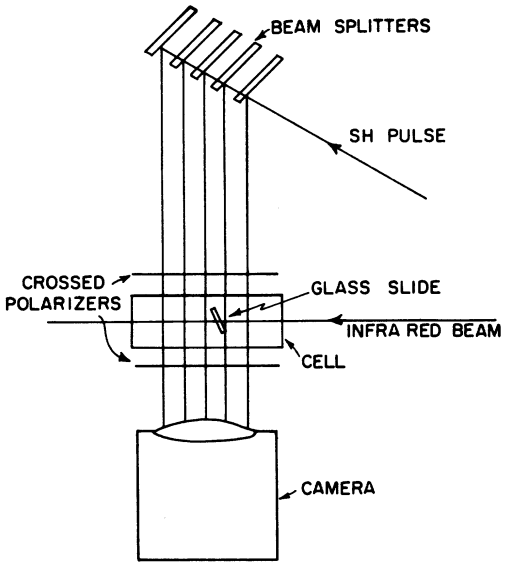

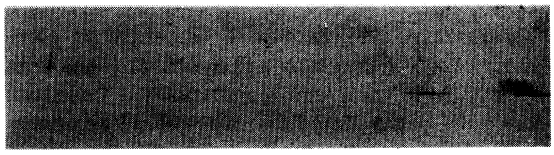

b

FIG. 9. Measurement of the effects of a glass slide (linear medium) on the propagations of filaments in CS_2: (a) experimental apparatus, indicating changes from basic equipment; (b) glass-slide results.

to CS_2 ($n = 1.62$), and therefore should have little or no effect on the streak produced by a succession of moving focal points. Preliminary results of the present experiments are shown in Fig. 9, where the effect of the glass slide [Fig. 9(b)] can be compared with regular birefringence data as shown in Fig. 6. After the slide, the filamentary streaks are barely visible, although present in the third beam, while in both beams 4 and 5, no detectable filament is present. This is in marked contrast to the set of pictures with no glass slide. The decrease in transmitted SH intensity through the filament region of beam three is about one order of magnitude, and it is difficult to estimate the new filament beam diameter.

The effect of a 1-mm-thick glass slide on the propagation of a small-scale filament provides evidence that there is some degree of beam confinement in the self-focused region of a picosecond pulse, as is predicted by the transient theory. The glass slide will cause the light contained in the region of small diameter in the tail of the pulse to diffract more rapidly than the light nearer the front of the pulse. After the glass slide, the light in the fore part of the pulse will again create a focusing effect on the light in the tail and will have its greatest effect on rays in the original filament that were closest to being paraxial. Because of the large cone angle of the light in the rear of the pulse resulting from diffraction in the linear medium, only a small fraction of the light contained in the original filament can participate in the refocusing process. A study of the intensity and diameter of the filaments after the glass slide as a function of glass thickness could provide more information on the shape of the pulse that leads to the filament.

In most of the birefringence data presented here, the number of filaments in the beam varies between two and ten. In some cases a single filament was obtained. Recently, the multiple filaments generated by Q-switched-laser pulses have been demonstrated to be correlated with instantaneous hot spots in the beam.[25]

To investigate this effect, the number of filaments produced in CS_2 was studied for various beam qualities and diameters. A telescope consisting of a +40-cm lens and a +10-cm lens with an aperture at their common focus was used to reduce the beam diameter. The diameter of the aperture between the lenses was varied between 0.38 and 4 mm. The diameter of the spot at the focus of the 40-cm lens was about 0.8 mm, which exceeds the spot size of 0.08 mm expected for diffraction-limited divergence. The large divergence is caused by the beam-processing optics. The diameter of the telescoped beam in the absence of the aperture was about 4 mm. After the telescope, a second aperture was used to vary the diameter of the collimated beam from 0.5 to 2 mm. Both apertures were positioned in the beam at each diameter to have maximum transmission.

The results of these experiments show that when the aperture within the telescope was removed, the number of filaments which were observed decreased as the diameter of the aperture after the telescope was reduced. However, even at 0.5 mm, several filaments were usually observed. When the aperture inside the telescope was reduced below about 1 mm, however, and the resultant collimated beam was subsequently apertured to about 2 mm in diameter, sufficient mode selection was present for single filaments to be observed some of the time in CS_2. By reducing the aperture inside the telescope to 0.38 mm and setting the aperture after the telescope to a diameter of 1 mm, single filaments were consistently observed in CS_2, as shown in Fig. 6. In materials with smaller Kerr constants than CS_2, single filaments could be observed with less stringent beam processing. Although the use of a 0.38-mm-diam aperture inside the telescope did not completely diffraction limit the beam, its divergence was substantially reduced. Careful positioning of both apertures to select the best part of the beam after the telescope reduced the spatial structure further to where a single filament could always be generated. In addition to reducing the beam diameter, the use of the apertures reduced the total power entering the cell, thus decreasing the probability of forming multiple filaments.

The birefringence technique discussed here provides an excellent method of detecting fluctuations in the beam intensity not only in space, but also in time. It was shown in Ref. 25 that a beam which has a smooth temporal and spatial profile when averaged over the entire pulse can show considerable local structure, when measured with sufficient temporal and spatial resolution. Since the self-focusing process accentuates small varia-

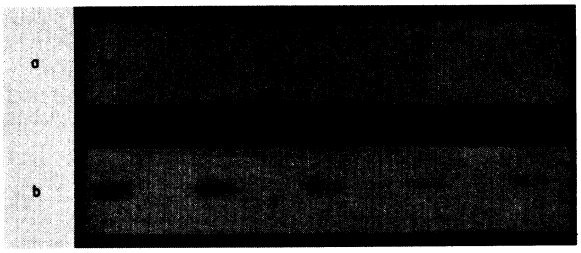

FIG. 10. Birefringence traces in CS_2 showing that several filaments can form at different times in a single laser pulse.

tions in the beam intensity, the presence of small local instantaneous hot spots can be detected using self-focusing for diagnostics purposes. In addition, the time dependence of these local hot spots can also be studied when a much shorter duration pulse is used in the probe beam. Figure 10 shows two birefringence traces from CS_2 in which multiple filaments were observed. If the filaments all arose from the same spatial and temporal portion of the infrared pulse, they would have appeared to start at the same spatial position in the SH probe beam. Figure 10 shows a random distribution of starting positions for the filaments. When correlated with end-camera pictures, the spatial and temporal variations of the local hot spots in the beam can be separated, since the propagation time of the compressed SH probe pulse across the infrared beam is well known.

Self-focusing in CS_2 was also studied for the case where the infrared beam is focused by an external lens before entering the cell.[40] Focal lengths of 20, 40, and 100 cm were used, and typical results are shown in Fig. 11. The pictures are taken between 0.5 and 4 cm in the cell, and the center of the geometric focal region is at the location of the third probing beam, 2.5 cm from the entrance window.

These results indicate that certain characteristics of self-focusing in collimated beams are accentuated in focused beams. Since CS_2 has a relatively low self-focusing threshold, focusing with a lens of less than about 80-cm focal length produces filaments within about 0.5 cm of the entrance window, as opposed to the 1.5 to 2 cm required for the appearance of filaments with a collimated beam. The filaments obviously can appear before the geometrical focus of the beam is reached, and also can extend several centimeters beyond the geometrical focus of the lens before disappearing. The distance over which the filaments are observed decreases considerably as the beam is focused more tightly. From Fig. 11, it can be seen that the filaments in CS_2 disappear in only 2 or 3 cm after the geometrical focus when the beam is focused with the shorter-focal length lenses. For longer-focal-length lenses, the behavior of the beam is essentially equivalent to the results for collimated beams. This is to

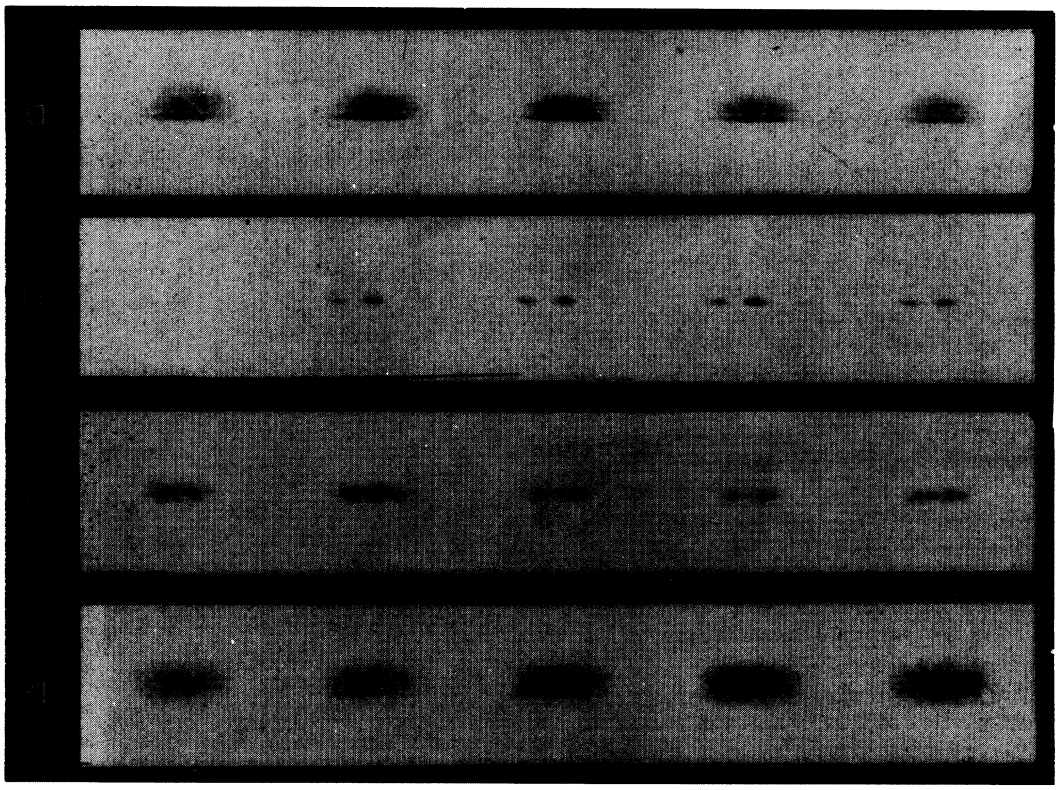

FIG. 11. Observation of self-focusing in externally focused beams in CS_2 between 0.5 and 4 cm into cell: (a) collimated beam, (b) infrared beam focused with 20-cm lens at the position of the third probing beam, (c) Ir beam focused with 40-cm lens at the position of the third probing beam, and (d) Ir beam focused with 100-cm lens at the position of the second probing beam.

be expected since, with the parameters of the present beam, the depth of the focal volume produced by a 1-m focal-length lens was measured to be about 15 cm. The contrast between the SH probe light transmitted due to the filament and that due to the background is not significantly different for the focused beams and the collimated beams in either CS_2 or benzene. Consequently, the maximum index change is about the same in both collimated and focused beams.

These results are consistent with predictions based on the transient calculations, since the initial convergence contributes an ever increasing index change for the back of the pulse, thus decreasing the minimum self-focusing length. On the other hand, after the focus the high divergence of the beam reduces the magnitude of δn, which is seen at the back of the pulse where the filament exists, and thus the filament diffracts away more rapidly than for collimated excitation. Also, there is clearly a limiting mechanism which restricts the intensity that does not require long propagation path lengths to become effective.

The interpretations of the major results of this section will be deferred until Sec. IV so that the spectral broadening results can be presented, thus allowing the more complete picture to be discussed at that time.

III. SPECTRAL BROADENING

The spectral content of the light in the filaments was measured by imaging the end of a 6-cm cell, containing various self-focusing materials, on the slit of a Spex $\frac{3}{4}$-m spectrograph. A 10-cm focal-length lens at a magnification of 10:1 was used. The light which did not self-focus was blocked by a 1-mm-diam stop, which was placed at the focus of the imaging lens. In addition, a Corning CS 7-56 filter was used to block the visible light from entering the spectrograph. The spectra were recorded on hypersensitized Kodak I-Z spectroscopic plates.

Typical spectra obtained for CS_2, toluene, benzene, and nitrobenzene are shown in Fig. 12. Figure 13 shows microdensitometer traces of the filament in CS_2 and toluene made directly from the plate, and Fig. 14 shows the same traces after they have been corrected for the spectral characteristics of the Kodak I-Z plates and the transmission characteristics of the Corning CS 7-56 filter.

The spectra, for all the materials studied here, show an interference pattern which is characteristic of a self-phase-modulated pulse, with the intensity and spacing of the interference maxima increasing with distance from the center frequency of the laser.

For the experimental spectra presented in Figs. 12–14, the average spacing between the modulation peaks is approximately 50 cm^{-1}. This value is most accurately determined from the spectra which contain many interference maxima, such as those shown for toluene and CS_2, but is also applied fairly well to the spectra from nitrobenzene and benzene.

The extent of the broadening varies over a large range from one filament to the next for a given material, and from one material to another. The largest broadening was consistently seen in CS_2, with spectra extending usually between 500 and 1000 cm^{-1} on either side of the laser frequency ("frequency" here measured in wave-number units).

The maximum broadening in toluene was less, with the spectra generally extending between 300 and 500 cm^{-1} on either side of the laser frequency. The extent of the broadening in benzene and nitrobenzene was in the vicinity of 200–300 cm^{-1} on

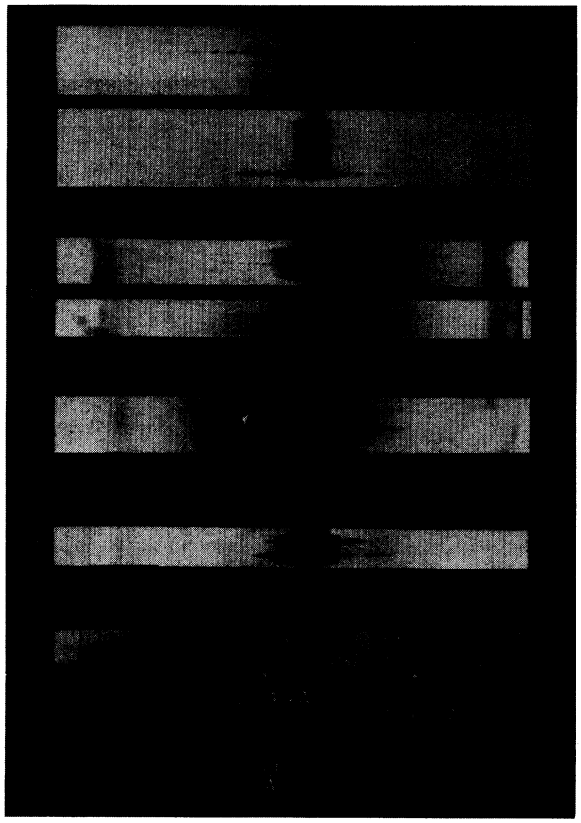

FIG. 12. Spectra of self-focused filaments obtained by imaging the end of a 6-cm cell onto the slit of a Spex $\frac{3}{4}$-m spectrograph with a magnification of 10:1: (a) CS_2, (b) toluene, (c) benzene, (d) nitrobenzene, and (e) Hg calibration.

either side of the laser frequency. Note that the degree of symmetry of the broadening on the Stokes and anti-Stokes side of the laser is quite high for all of the materials studied. The number of peaks and extent of the spectra is approximately the same on each side of the laser frequency for most filaments, although occasional filaments show a small degree of asymmetry in the extent of the broadening.

The relative amount of energy contained in the upshifted and downshifted light is more difficult to determine because of the complications introduced by the spectral characteristics of the plates and the filter and by the unshifted background, which resulted from the unfocused laser light. However, from the corrected densitometer traces of Fig. 14, the ratio of the energy contained in the Stokes side to that contained in the anti-Stokes side of the spectrum is estimated to be between 1 and 2. The degree of symmetry exhibited by

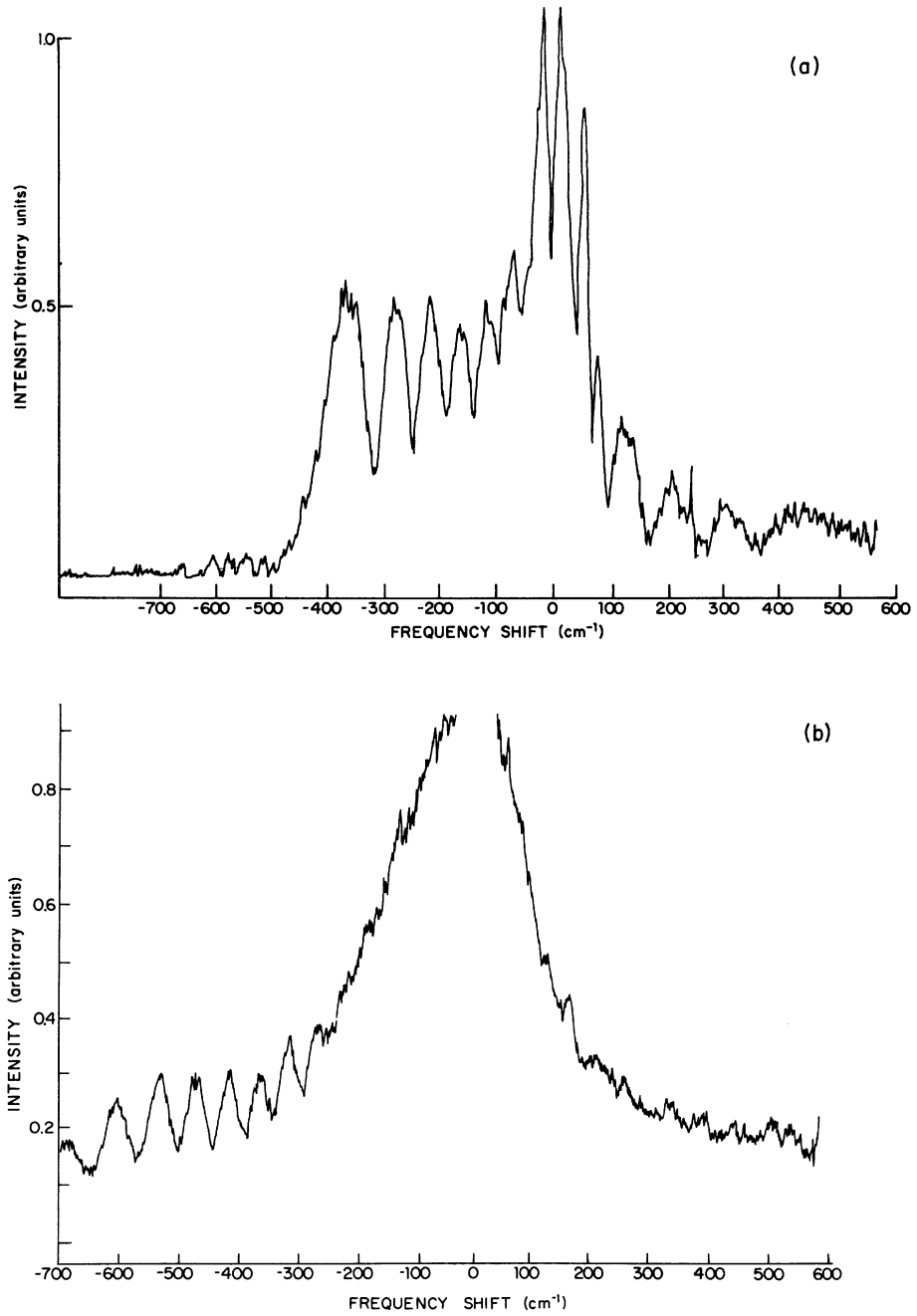

FIG. 13. Microdensitometer traces of the spectra shown in Fig. 12 for (a) CS_2 and (b) toluene.

these spectra is much greater than that shown by the filaments generated with multimode Q-switched[17,18] lasers. The present spectra are more nearly in agreement with the results obtained with mode-locked ruby lasers,[11] although quantitative differences exist between the spectra generated with the two different mode-locked laser systems.

Frequency-broadened spectra such as those described have been successfully explained using the theory of self-phase modulation for plane-wave propagation.[17,19] The results of the recent numerical calculations show that the actual filament does not assume uniform rod shape; but rather has variations in its radius and intensity as it propagates.[16] However, because of the following two reasons, the plane-wave model can describe many aspects of the spectrum. First, the filament travels a distance in the medium which is many times its linear-diffraction length without changing its gross characteristic. Therefore in an approximate sense, it is a one-dimensional object. Second, the many features of the frequency spectrum are insensitive to the exact shape of the filament. These are, for example, the average spacing of the peaks of the modulated spectrum, the ratio of the energy and the relative extent of the broadening between Stokes and the anti-Stokes sides. The average spacing of the modulation can be used to estimate the duration of the pulse in the filament, provided the spectrum does not have a strong central component.

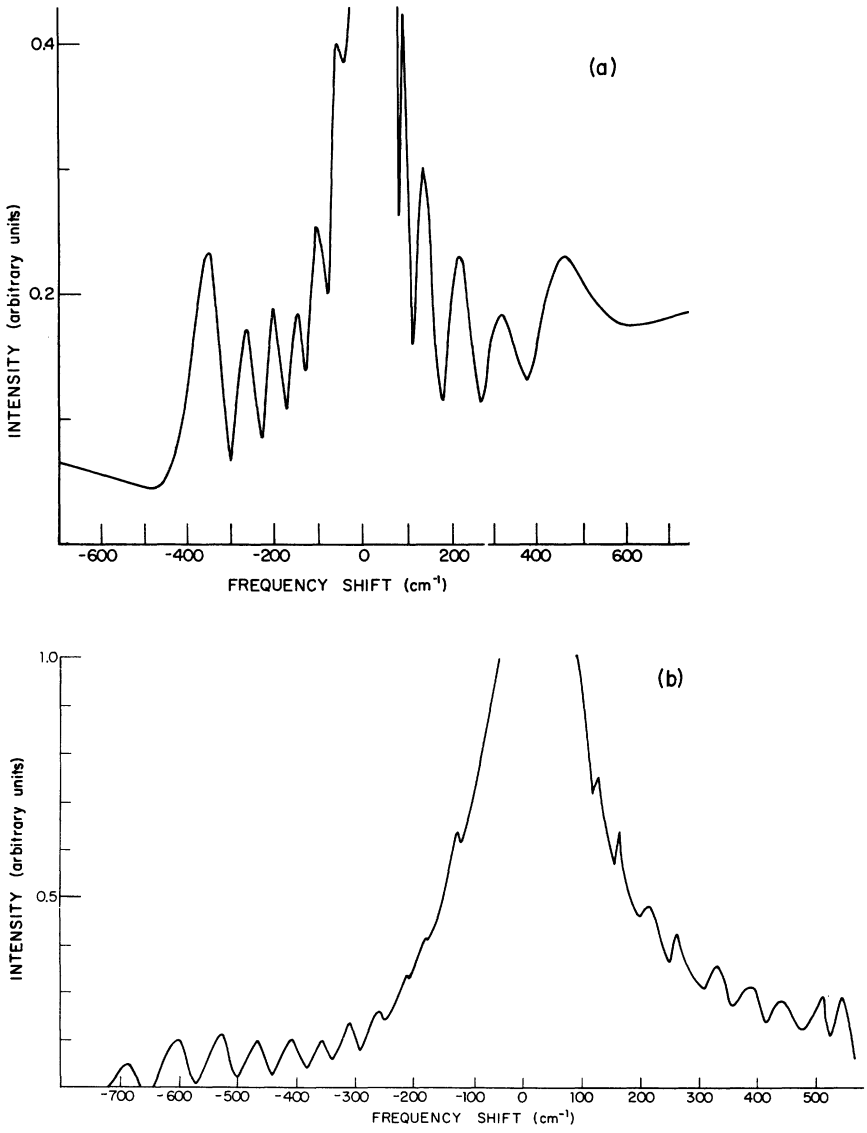

FIG. 14. Microdensitometer traces of Fig. 13 after corrections for the special characteristics of the Kodak I-Z plates: (a) CS_2 and (b) toluene.

The ratios of the intensity and extent of the spectrum on either side of the laser center frequency are related to the asymmetry of the pulse shape and the relaxation time of δn in this model. One has to be careful in discussing the features of the anti-Stokes side. The main contribution to the anti-Stokes side comes from the latter part of the filament, which is often relatively unstable and varies according to the cutoff mechanism of the filament. Let us now discuss what kind of mechanisms can induce the observed spectrum in the one-dimensional model. We assume for the response of δn an equation of the more general form

$$\tau_2^2 \frac{\partial^2}{\partial t^2} \delta n + \tau_1 \frac{\partial}{\partial t} \delta n + \delta n = n_2 |E|^2 . \tag{3}$$

Further assuming that the pulse-envelope distortion is small, as in the discussion in Sec. I, the additional phase change θ of the optical field caused by δn in Eq. (3) is

$$\theta = 2\pi \delta n L/\lambda , \tag{4}$$

where λ is the vacuum wavelength and L is the propagation length of the filament. The spectrum can be then obtained by Fourier transforming the field $Ae^{i\theta}$.

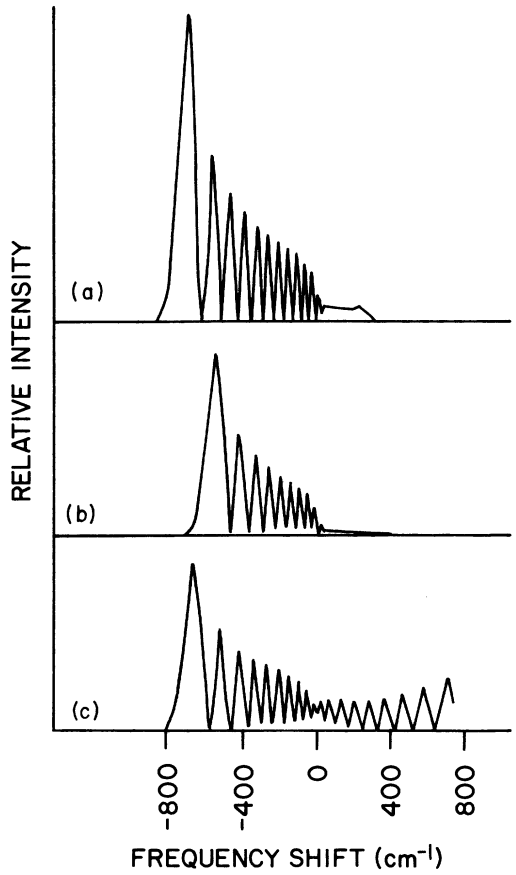

FIG. 15. Theoretical spectra calculated using the wave-guide model corresponding to (a) orientational effect in CS_2, $\tau_2 = 0$, $\tau_1 = 2T$; (b) librational effect in CS_2, $\tau_2 = 0.26T$ and $\tau_1 = 0.46T$; and (c) electronic effect, $\tau_1 = \tau_2 = 0$. T is the duration of the laser pulse as determined from the experimental spectra of Fig. 12.

In Fig. 15 we show three cases of the response, $\tau_2 = 0$ and $\tau_1 = 2T$, $\tau_2 = 0.26T$ and $\tau_1 = 0.46T$, and $\tau_1 = \tau_2 = 0$, where T is the duration of the pulse. The pulse envelope for the calculations is assumed to be Gaussian with a duration of 1 psec. The first case is appropriate for the orientational Kerr effect, where the value of τ_1 corresponds to that of CS_2. The next one approximates the librational response for comparison purposes. The numbers for this last case are taken from the observed depolarized Rayleigh scattering in the far-Rayleigh-wing, assuming the shoulder around 13 cm^{-1} is due to that mechanism.[41] The last corresponds to a fast response such as the electronic Kerr effect. The pulse-envelope duration of 1 psec was arrived at by adjusting the duration in order to obtain a 50 cm^{-1} average spacing between the modulation peaks, which corresponds to the experimental results shown in Figs. 12–14. It can be seen immediately that for this choice of parameters only the electronic response generates enough anti-Stokes light to be comparable to the experimental spectra. This result should be contrasted with the interpretations given to the spectra obtained in CS_2 with both multimode Q-switched,[7,9] and mode-locked ruby lasers.[11] A sufficient amount of spectral asymmetry was observed so that the results agreed with the predictions of an orientational response for the multimode laser. With a mode-locked ruby laser,[11] a filament pulse duration of 2.3 psec was obtained, which allowed an interpretation in terms of a librational response in CS_2.

It is possible to estimate an upper limit of the magnitude of τ_1 and τ_2 from a set of parametrized calculations of the frequency broadening. Assuming that each point of the pulse has an (instantaneous) frequency $d\theta/dt$, we calculated the ratio of the extent of the Stokes to the anti-Stokes frequency broadening $\omega_S(\max)/\omega_{AS}(\max)$, and the ratio of the energy content on the Stokes to anti-Stokes side of the spectrum, W_S/W_{AS}, in terms of the input pulse temporal asymmetry for an orientational response ($\tau_2 = 0$, $\tau_1 = T$). A section of these curves in the vicinity $t = 0.1T$ are shown in Fig. 16 for a Gaussian pulse of the form

$$E(t) = \begin{cases} E_0 e^{-t^2/\tau_1^2}, & T < 0 \\ E_0 e^{-t^2/\tau_2^2}, & T > 0 \end{cases}$$

$$t_p = T_1 + T_2 .$$

The dotted lines indicate the regions of the curves that can describe the experimental results shown in Figs. 12–14. The limits on the pulse asymmetry obtained in this manner are $0.6 < T_2/T_1 < 1.3$. The relaxation time τ is determined to be less than one-tenth the pulse duration and therefore has an upper limit of 0.1 psec for a pulse duration of 1 psec. The predicted degree of spectral asymmetry for the situation in which $\tau = 2t_p$ (appropriate for CS_2 when $t_p = 1$ psec) agrees with the numerical results of the transient theory[16] when the filament propagates over a distance which is much longer than that required for it to form. This result is rather surprising, since the propagation data all point to the dominance of the orientational mechanism in the filament formation. The implications of this result will be discussed further in Sec. IV.

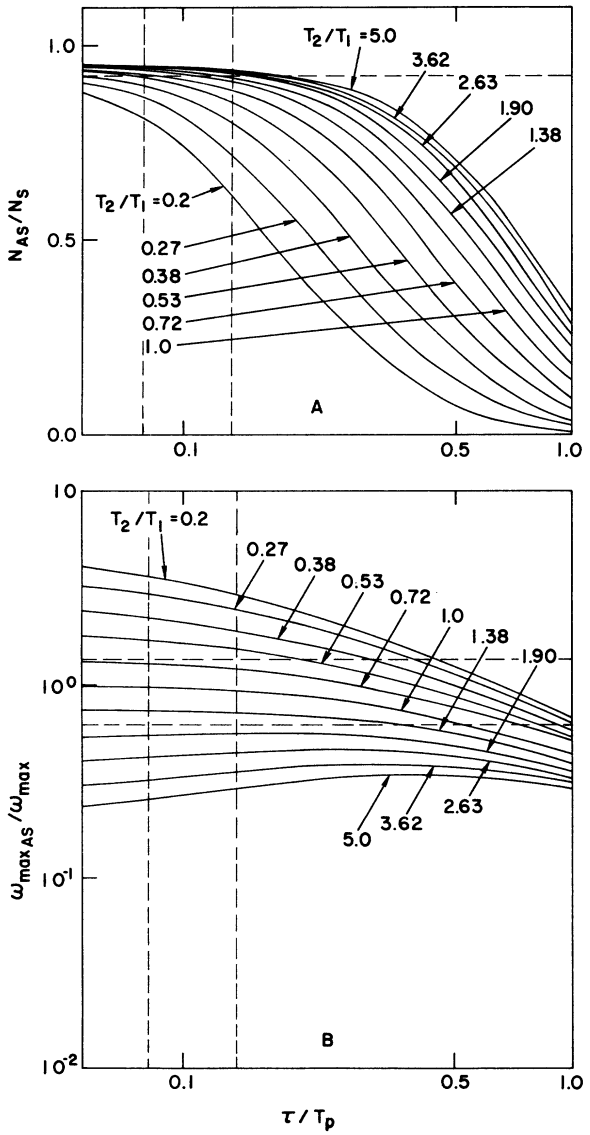

FIG. 16. Parametric calculation using the wave-guide model of (a) ratio of number of anti-Stokes peaks to number of Stokes peaks, and (b) extent of Stokes broadening to anti-Stokes broadening for various pulse asymmetries and dielectric relaxation times. The dotted lines indicate the regions which can be used to explain the experimental spectra.

IV. DISCUSSION AND CONCLUSIONS

Estimates of the duration of the pulse in the filament were made from both the spatial propagation and the spectral measurements. In the case of the spatial-propagation measurements, the pulse duration was estimated from the birefringence measurements in CS_2. Under the assumptions of an orientational Kerr relaxation time of 2.3 psec, which contributes a duration of about 1.25 psec/Np to the birefringence streak, and a SH probe-beam duration of about 1 psec, an estimated duration of 1 psec for the fundamental intensity accounts quite well for the observed duration of the birefringence streak. This pulse is significantly shorter than the 5-psec envelope at the entrance to the cell, as determined by TPF measurements.

The duration of the infrared pulse in the high-intensity region was also estimated from the average spacing of the modulation peaks in the frequency-broadened spectra. In most of the materials studied, the average spacing of these peaks was 50 cm^{-1}. Using results of numerical calculations, this spacing was related to a pulse duration of 0.9 psec, again consistent with the result from the spatial-propagation studies.

The applicability of the transient theory to the present work was directly determined from the measurements of the lifetime of the optical anisotropy in nitrobenzene and toluene. These results showed that the dominant response of the nonlinear index in these materials is due to the orientational Kerr effect.[31] It has been suggested that faster mechanisms, such as electronic or librational Kerr effects may be important in the self-focusing of picosecond pulses in these materials.[7,11] If an electronic effect with a response time of the order of 10^{-15} sec were dominant, the infrared pulse is expected to self-focus according to the quasi-steady-state theory of moving focal points. Because of the absence of stimulated Raman scattering in the present experiments, the backward-moving focal point, if present, would not be expected to be terminated, as is the case in experiments done with longer pulses. Therefore, the presence of both focal points should be evident in the birefringence track, appearing as

two distinct spots when the two foci are separated by more than the duration of the SH probing pulse. These two spots should move apart steadily as the pulse propagates through the cell. On the basis of a purely electronic response, the two focal points should become distinct at about 8 cm from the entrance window for a pulse duration of 1-psec full width at half-maximum. For a pulse duration of 5 psec, they should separate even earlier. Careful probing of the birefringence signal in the region 5—12 cm into the cell has shown that only a single focal volume develops, and that it propagates with a constant duration for most of its existence. In addition, we should have observed a regular modulation pattern in the frequency spectrum with a period characteristic of the time between the two focal points. Consequently, we conclude that the faster mechanisms do not play a dominant role in the present self-focusing experiments.

In addition to comparing the time response of these effects, we have also investigated the magnitudes of the electronic and librational responses relative to the orientational effect. In Fig. 17, the ratio of the values of the electronic nonlinearity n_2^e to the orientational nonlinearity n_2^0, which is required to produce an equal refractive index change δn, is shown as a function of time and relaxation time for a 1-psec pulse. For the present materials, the ratio n_2^e/n_2^0 is expected to be less than 0.01, as is indicated by the shaded region of the figure. For the case of $\tau = 2.0$ psec, appropriate for CS_2, the orientational effect can be seen to dominate for all except the very early portions of the pulse. It should be remembered that the 1-psec pulse duration applies only after the filament has formed. The electronic effect has even less significance for the longer pulse, which exists before the beam completely self-focuses. Similar calculations comparing the librational and orientational Kerr effects in CS_2, where a good deal of spontaneous scattering data involving these processes exists, indicates that the orientational Kerr effect is always larger than the librational effect for pulses of 1-psec duration.

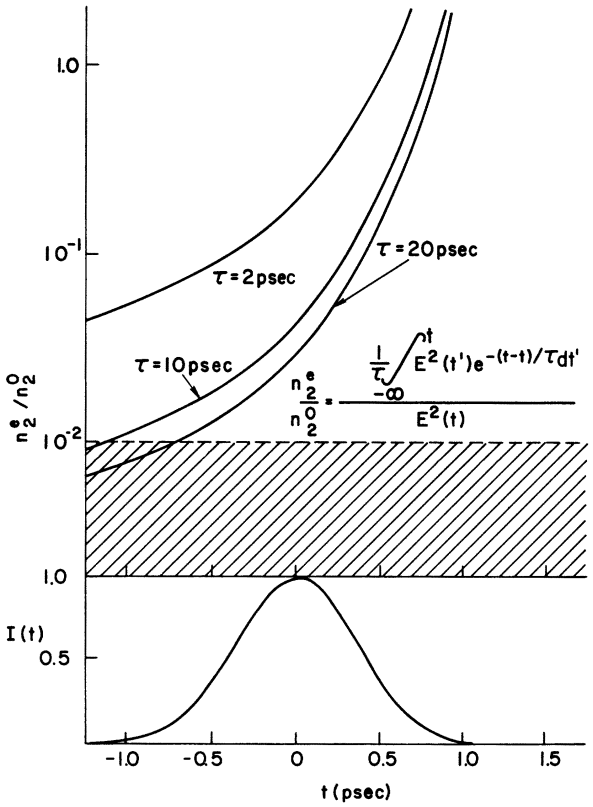

FIG. 17. Comparison of values of electronic nonlinearity n_2^e and orientational nonlinearity n_2^0 that are required to produce identical refractive index changes as a function of time during the laser pulse, shown at the bottom. The curves correspond to (a) CS_2, $\tau/t_p = 2$; (b) toluene, $\tau/t_p = 10$; and (c) nitrobenzene, $\tau/t_p = 50$; where t_p is the laser pulse duration.

Most of the spectral results are in reasonable agreement with the prediction of the transient theory of a filament with a 1-psec duration that propagates for many centimeters. The observed symmetry of the spectra, however, can be explained by n_2 effects only on the basis of a fast electronic response, but not a slow orientational response, as was shown in Sec. III.

It may be possible to reconcile this result with the overwhelming evidence that the major effect here is transient self-focusing due to an orientational Kerr effect if the driving term of the parabolic Maxwell equation [Eq. (1)] is insufficient to describe the evolution of the spectral broadening; that is, additional terms must be added to the Maxwell equations to incorporate other pulse-propagation features. If linear dispersion is considered, a phase mismatch exists in the forward direction for different frequencies, possibly causing self-steepening and allowing exponential gain[19] to occur for both upshifted and downshifted light. Rough estimations indicate that sufficient forward gain exists at field intensities of ≈ 100 GW/cm^2 for the upshifted intensity to reach 90% of the downshifted intensity after a few millimeters.[42] This coupling may also account for the symmetry of the observed spectra. For lower intensities, sufficient gain might not exist, allowing some filaments to be asymmetrically broadened. In addition off-axis phase matching of a four-photon process can take place within the filament.[43] This process can pump light out of the high-intensity region and may contribute to

the light which is observed radiating from the filaments in the interior of the cell. It may also be partially responsible for the depletion of the filament intensity sufficient to cause the filaments to disappear after about 15 cm of propagation path length. Otherwise, we would have to postulate that the initial spatial structure, from which the self-focusing occurred, would have to be $< 100\ \mu$ in order to account for the filament diffracting due to precursor diffraction from a few microns diameter up to $> 100\ \mu$ for a 15-cm propagation path.

Additional effects, such as avalanche breakdown[44] or backward-stimulated Raman or Rayleigh scattering,[45] have been recently proposed as mechanisms which can limit the diameter of the filaments. Since the broadening of the spectrum on the anti-Stokes side is very sensitive to the behavior of the phase and the intensity in the second half of the pulse, these limiting mechanisms may also play a role in determining the degree of spectral symmetry involved. In such a situation, careful study of the anti-Stokes spectrum may reveal information concerning the mechanisms which contribute to this limitation of the filament diameters.

ACKNOWLEDGMENTS

The authors would like to gratefully acknowledge Professor Bloembergen's support and the free giving of his time for discussions during this work. We also acknowledge helpful discussions with most of the people working in the field. We particularly thank P.L. Kelley, Y.R. Shen, E. Courtens, J. Fleck, T.K. Gustafson, A.M. Prokhorov, J. Marburger, M.J. Colles, and D. Pohl.

---

*Work submitted as partial fulfillment of the Ph.D. requirement for one of the authors (J. Reintjes) at Harvard University, 1971.

†Work at Harvard supported by the U. S. Army Research Office, Durham, under Contract No. DAHC-04-68-C-0037, the Joint Services Electronics Program under Contract No. N00014-67-A-0298-0006, and the National Aeronautics and Space Administration under Grant No. NGR 22-007-117.

‡National Science Foundation; present address: IBM Watson Research Center, Yorktown Heights, N. Y. 10598.

§Address during the latter part of this work and present address: Lawrence Livermore Laboratory, Livermore, Calif. 94550. The latter part of this work was partially supported under the auspices of the U. S. Atomic Energy Commission.

‖Address during the latter part of this work, IBM Research Laboratory, Zurich, Switzerland. Present address: Tokyo University, Department of Electrical Engineering, Tokyo, Japan.

[1]For a review of the earlier work, see S. A. Akhmanov, A. P. Sukhorukov, and R. V. Khokhlov, Usp. Fiz. Nauk **93**, 19 (1967) [Sov. Phys.–Usp. **93**, 609 (1968)].

[2]See, for example, R. G. Brewer, J. R. Lifsitz, E. Garmire, R. Y. Chiao, and C. H. Townes, Phys. Rev. **166**, 326 (1968), and references therein; V. V. Korobkin and R. V. Serov, Zh. Eksp. Teor. Fiz. Pis'ma Red. **6**, 642 (1967) [JETP Lett. **6**, 135 (1967)]; E. Garmire, R. Y. Chiao, and C. H. Townes, Phys. Rev. Lett. 16, 347 (1966).

[3]The following publications contain most of the important recent theoretical results plus references to earlier work: A. A. Abromov, V. N. Lugovoi, and A. M. Prokhorov, Zh. Eksp. Teor. Fiz. Pis'ma Red. **9**, 675 (1969) [JETP Lett. **9**, 419 (1969)]; M. M. T. Loy and Y. R. Shen, Phys. Rev. Lett. **22**, 994 (1969); J. P. Taran and T. K. Gustafson, IEEE J. Quantum Electron. **QE-5**, 381 (1969).

[4]M. M. T. Loy and Y. R. Shen, Phys. Rev. Lett. **25**, 1333 (1970).

[5]V. V. Korobkin, A. M. Prokhorov, R. V. Serov, and M. Ya. Schelev, Zh. Eksp. Teor. Fiz. Pis'ma Red. **11**, 153 (1970) [JETP Lett. **11**, 94 (1970)]; N. I. Lepatov, A. A. Manenkov, and A. M. Prokhorov, Zh. Eksp. Teor. Fiz. Pis'ma Red. **11**, 444 (1970) [JETP Lett. **11**, 300 (1970)]; R. L. Carman, A. Mooradian, P. L. Kelley, and A. Tufts, Appl. Phys. Lett. **14**, 136 (1969).

[6]J. P. McTague, C. H. Lin, T. K. Gustafson, and R. Y. Chiao, Phys. Lett. A **32**, 82 (1969); R. R. Alfano and S. L. Shapiro, Phys. Rev. Lett. **24**, 1217 (1970).

[7]R. G. Brewer and C. H. Lee, Phys. Rev. Lett. **21**, 267 (1968); R. G. Brewer and J. R. Lifsitz, Phys. Lett. **23**, 79 (1966).

[8]R. L. Carman, M. E. Mack, and J. Reintjes, in Proceedings of the Sixth International Quantum Electronics Conference, Kyoto, Japan, 1970, paper 9-12 (unpublished); S. Saikan and H. Takuma, in Proceedings of the Sixth International Quantum Electronics Conference, Kyoto, Japan, 1970, paper 9-3 (unpublished).

[9]R. R. Alfano and S. L. Shapiro, Phys. Rev. Lett. **24**, 592 (1970).

[10]M. E. Mack, R. L. Carman, J. Reintjes, and N. Bloembergen, Appl. Phys. Lett. **16**, 209 (1970).

[11]R. Polloni, C. A. Sacchi, and O. Svelto, Phys. Rev. Lett. **23**, 690 (1969); R. Cubeddu, R. Polloni, C. A. Sacchi, and O. Svelto, Phys. Rev. A **2**, 1955 (1970).

[12]P. L. Kelley, Phys. Rev. Lett. **15**, 1005 (1965).

[13]E. L. Dawes and J. H. Marburger, Phys. Rev. **179**, 862 (1969).

[14]S. A. Akhmanov, A. P. Sukhorukhov, and R. V. Khokhlov, Zh. Eksp. Teor. Fiz. **51**, 296 (1966) [Sov. Phys.-JETP **24**, 198 (1967)].

[15]J. A. Fleck, Jr. and P. L. Kelley, Appl. Phys. Lett. **15**, 313 (1969); V. A. Aleshkevich, S. A. Akhmanov, A. P. Sukhorokov, and A. M. Khachumyan, Zh. Eksp. Teor. Fiz. Pis'ma Red. **13**, 55 (1971) [JETP Lett. **13**, 36 (1971)].

[16]F. Shimizu, Phys. Rev. Lett. (to be published); J. A. Fleck, Jr. and R. L. Carman, Appl. Phys. Lett. **20**, 290 (1972).

[17]F. Shimizu, Phys. Rev. Lett. **19**, 1097 (1967).

[18]R. L. Carman, J. Hanus, and D. L. Weinberg, Appl. Phys. Lett. **11**, 250 (1967).

[19]T. K. Gustafson, J.-P. Taran, H. A. Haus, J. R. Lifsitz, and P. L. Kelley, Phys. Rev. **177**, 306 (1969).

[20]M. M. T. Loy and Y. R. Shen, Phys. Rev. Lett. **22**, 994 (1969).

[21]Foci can travel faster than the velocity of light, implying that the light from an earlier focus does not affect the light about to go through a focus.

[22]J. Reintjes, R. L. Carman, F. Shimizu, and H. Furumoto, in

Proceedings of the Sixth International Quantum Electronics Conference, Kyoto, Japan, 1970, paper 9-4 (unpublished).
[23]See, for example, R. L. Carman, F. Shimizu, C. S. Wang, and N. Bloembergen, Phys. Rev. A **2**, 60 (1970), and reference therein.
[24]F. Shimizu and B. Stoicheff, IEEE J. Quantum Electron. **QE-5**, 544 (1969).
[25]S. C. Abbi and H. Mahr, Phys. Rev. Lett. **26**, 604 (1971).
[26]R. R. Alfano and S. L. Shapiro, Phys. Rev. A **2**, 2376 (1970).
[27]S. L. Shapiro, J. A. Giordmaine, and K. W. Wecht, Phys. Rev. Lett. **19**, 1093 (1967).
[28]M. M. Maller and P. M. Rantzepis, Chem. Phys. Lett. **21**, 267 (1968).
[29]J. Reintjes and R. L. Carman (unpublished).
[30]E. B. Treacy, IEEE J. Quantum Electron. **QE-5**, 454 (1969); E. B. Treacy, Phys. Lett. A **28**, 34 (1968).
[31]J. Reintjes and R. L. Carman, Phys. Rev. Lett. **28**, 1697 (1972).
[32]Our measurement is in reasonably good agreement with previous measurements of Duguay and Hansen [Appl. Phys. Lett. **15**, 192 (1969)] in nitrobenzene of 32 ± 6 psec.
[33]R. W. Hellwarth, Phys. Rev. **152**, 156 (1966).
[34]R. W. Hellwarth, A. Owyoung, and N. George, Phys. Rev. A **4**, 2342 (1971).
[35]W. S. Gornall, H. E. Howard Loche, and B. P. Stoicheff, Phys. Rev. A **1**, 1288 (1970); J. P. McTague, P. A. Fleury, and D. B. Dupre, Phys. Rev. **188**, 303 (1969).
[36]T. K. Gustafson, P. L. Kelley, R. Y. Chiao, and R. G. Brewer, Appl. Phys. Lett. **12**, 165 (1968); A. Piekara, IEEE J. Quantum Electron. **QE-2**, 249 (1966).
[37]T. K. Gustafson and C. H. Townes, J. Quantum Electron. QE - 8, 587 (1972), Phys. Rev. A **6**, 1959 (1972).
[38]M. M. Denairez and J.-P.Taran, Appl. Phys. Lett. **14**, 205 (1969).
[39]E. Garmire, R. Y. Chiao, and C. H. Townes, Phys. Rev. Lett. **16**, 347 (1966).
[40]E. Courtens also performed some experiments with focused beams (private communication).
[41]S. L. Shapiro and H. P. Broida, Phys. Rev. **154**, 129 (1967); I. L. Febelinskii and V. S. Starunov, Appl. Opt. **6**, 1793 (1967).
[42]For example, see R. L. Carman, R. Y. Chiao, and P. L. Kelley, Phys. Rev. Lett. **17**, 128 (1966).
[43]Stimulated four-photon scattering has been reported previously in a number of materials, with both picosecond and nanosecond pulses. See: G. I. Zaitsev, Yu. I. Kyzylasov, V. S. Starunov, and I. L. Fabelinskii, Zh. Eksp. Teor. Fiz. Pis'ma Red. **6**, 695 (1967) [JETP Lett. **6**, 180 (1967)]; E. N. Grinberg, S. M. Ryvkin, I. M. Fisuman, and I. E. Yuroshetskii, Zh. Eksp. Teor. Fiz. Pis'ma Red. **7**, 324 (1968) [JETP Lett. **7**, 253 (1968)]; A. P. Veduta and B. R. Kirsanov, Zh. Eksp. Teor. Fiz. **56**, 1175 (1969) [Sov. Phys.-JETP **29**, 632 (1969)]; R. R. Alfano and S. L. Shapiro, Phys. Rev. Lett. **24**, 584 (1970); D. H. Auston, Appl. Phys. Lett. **18**, 249 (1971).
[44]N. Bloembergen, M. Bass, E. Yablonovitch, and D. Fradin (private communication); E. Yablonovitch and N. Bloembergen, Phys. Rev. Lett. **29**, 907 (1972).
[45]T. K. Gustafson and P. L. Kelley (private communication).

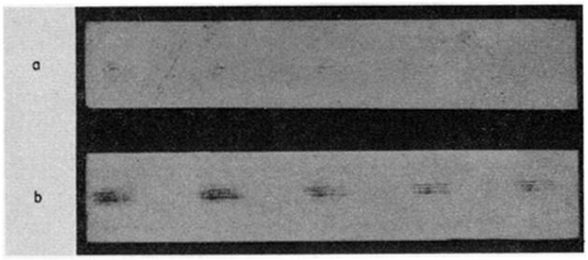

FIG. 10. Birefringence traces in CS_2 showing that several filaments can form at different times in a single laser pulse.

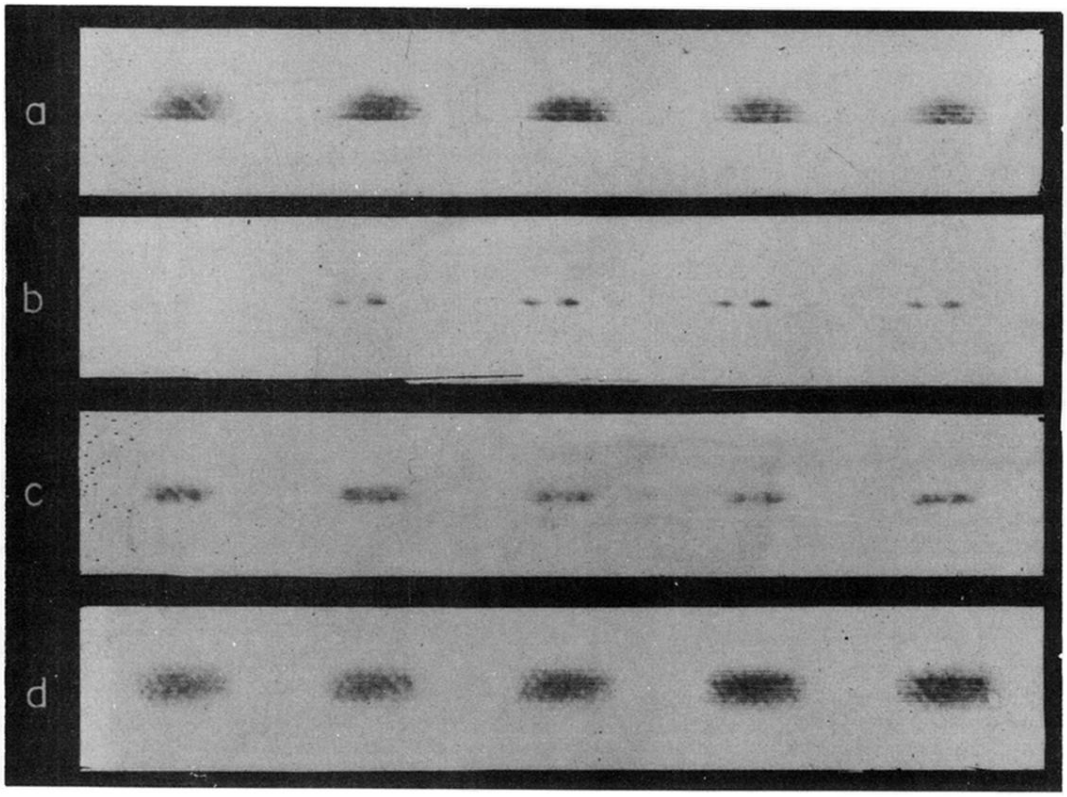

FIG. 11. Observation of self-focusing in externally focused beams in CS_2 between 0.5 and 4 cm into cell: (a) collimated beam, (b) infrared beam focused with 20-cm lens at the position of the third probing beam, (c) Ir beam focused with 40-cm lens at the position of the third probing beam, and (d) Ir beam focused with 100-cm lens at the position of the second probing beam.

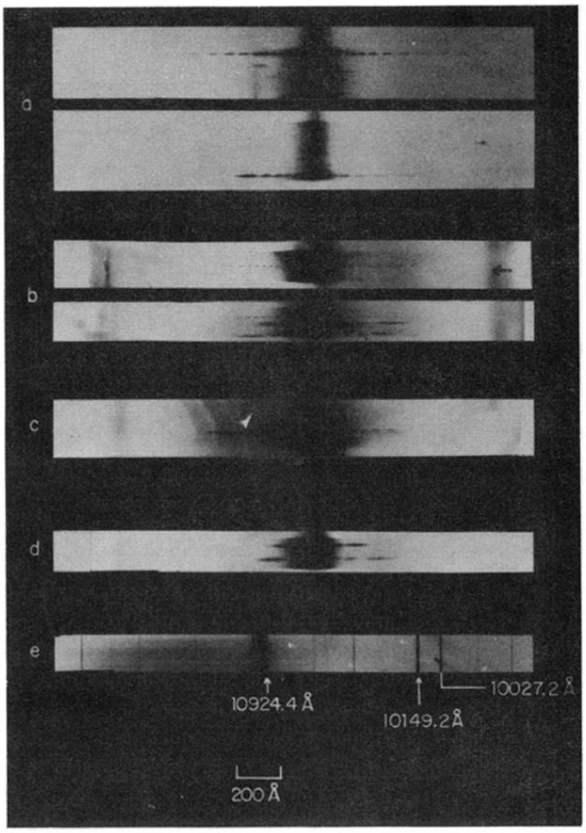

FIG. 12. Spectra of self-focused filaments obtained by imaging the end of a 6-cm cell onto the slit of a Spex $\frac{3}{4}$-m spectrograph with a magnification of 10:1: (a) CS_2, (b) toluene, (c) benzene, (d) nitrobenzene, and (e) Hg calibration.

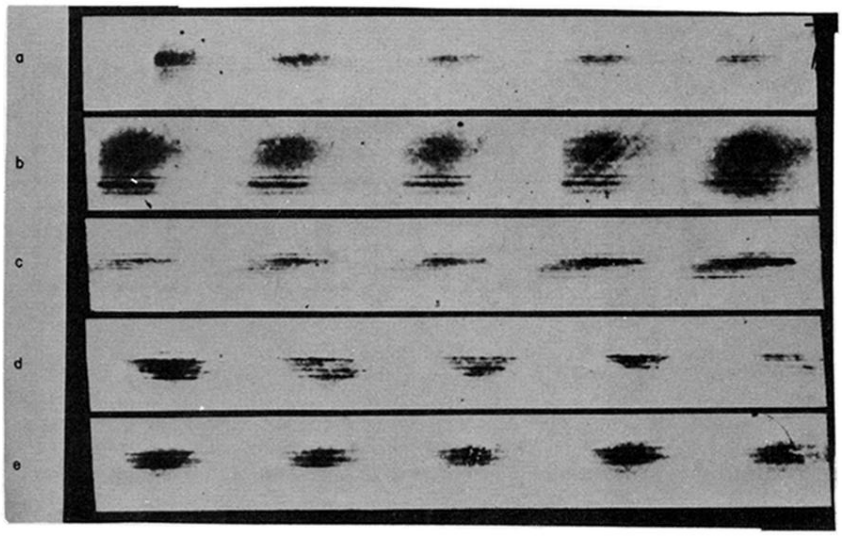

FIG. 2. Typical pictures of regions of induced birefringence in various parts of a 20-cm cell of CS_2. The infrared beam propagates from left to right. (a) 1.2 – 4.7 cm from entrance window; (b) 4.6 – 8.1 cm from entrance window; (c) 8 – 11.5 cm from entrance window; (d) 10.7 – 14.2 cm from entrance window; and (e) 15 – 18.5 cm from entrance window.

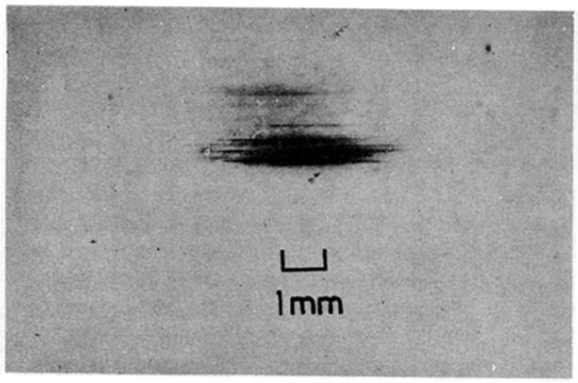

FIG. 3. Photograph of a single-probe beam taken 5 cm from the entrance window of a cell of CS_2 showing filamentary structure as small as 10 μ. Magnification of original photograph was 5× and the optical resolution was 10 μ.

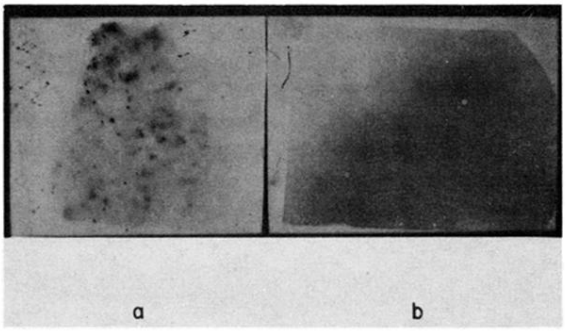

FIG. 4. Near-field pattern obtain with forward camera imaged (a) on a plane 13 cm before exit window of a 20-cm cell and (b) on a plane 7 cm before the exit window of the 20-cm cell.

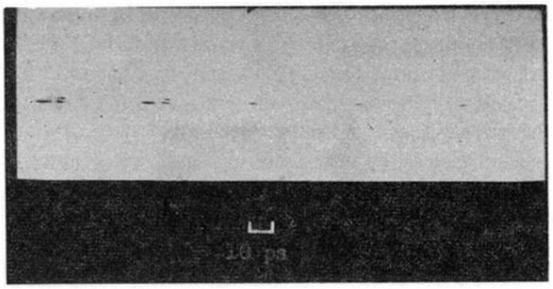

FIG. 6. Typical birefringence result in CS_2 obtained with the improved time resolution of the apparatus in Fig. 6. The reflections from the front and back surfaces of the beam splitter are clearly resolved in the first two beams.

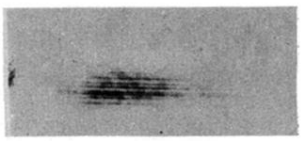

10 psec

a

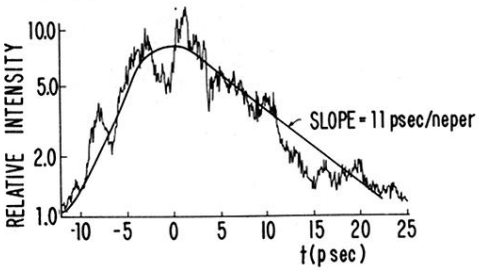

b

FIG. 7. Results of birefringence study in nitrobenzene: (a) photograph of filaments; (b) microdensitometer trace showing decay of birefringence with a time constant of 11 psec, corresponding to a lifetime of the nonlinear index of 22 ± 3 psec.

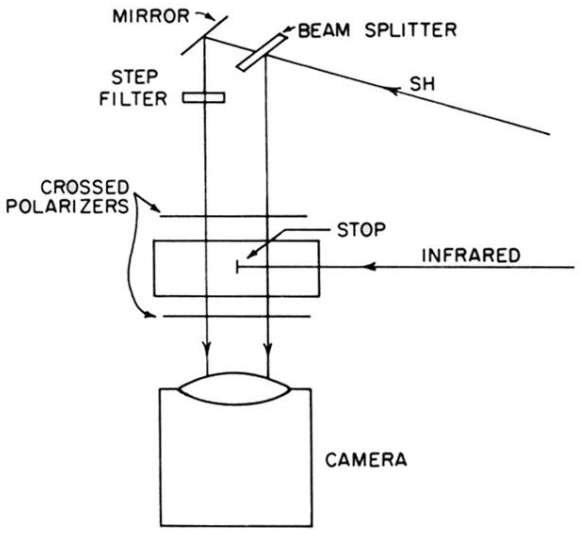

a

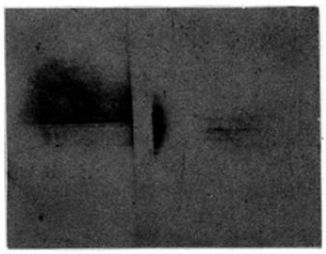

b

FIG. 8. Measurement of the maximum value of δn in the filaments: (a) experimental configuration, showing changes from basic experiments of Fig. 5 (elements in dotted box of Fig. 5 are changed to those shown); (b) results of birefringence measurements in CS_2.

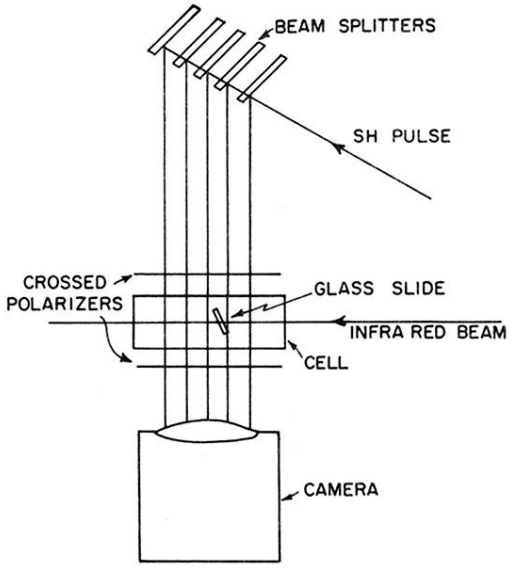

a

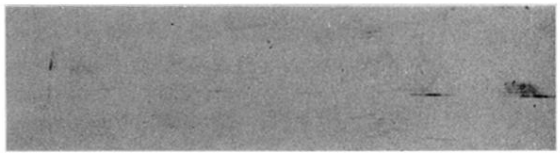

b

FIG. 9. Measurement of the effects of a glass slide (linear medium) on the propagations of filaments in CS_2: (a) experimental apparatus, indicating changes from basic equipment; (b) glass-slide results.